Climate forcing due to optimization of maximal leaf conductance in subtropical vegetation under rising CO_2

Hugo Jan de Boer[a,1], Emmy I. Lammertsma[b], Friederike Wagner-Cremer[b], David L. Dilcher[c,1], Martin J. Wassen[a], and Stefan C. Dekker[a]

[a]Environmental Sciences, Copernicus Institute for Sustainable Development, Utrecht University, 3508 TC, Utrecht, The Netherlands; [b]Palaeoecology, Laboratory of Palaeobotany and Palynology, Institute of Environmental Biology, Utrecht University, Budapestlaan 4, 3584 CD, Utrecht, The Netherlands; and [c]Department of Biology, Indiana University, Bloomington, IN 47405

Contributed by David L. Dilcher, January 24, 2011 (sent for review October 19, 2010)

Plant physiological adaptation to the global rise in atmospheric CO_2 concentration (CO_2) is identified as a crucial climatic forcing. To optimize functioning under rising CO_2, plants reduce the diffusive stomatal conductance of their leaves (g_s) dynamically by closing stomata and structurally by growing leaves with altered stomatal densities and pore sizes. The structural adaptations reduce maximal stomatal conductance (g_{smax}) and constrain the dynamic responses of g_s. Here, we develop and validate models that simulate structural stomatal adaptations based on diffusion of CO_2 and water vapor through stomata, photosynthesis, and optimization of carbon gain under the constraint of a plant physiological cost of water loss. We propose that the ongoing optimization of g_{smax} is eventually limited by species-specific limits to phenotypic plasticity. Our model reproduces observed structural stomatal adaptations and predicts that adaptation will continue beyond double CO_2. Owing to their distinct stomatal dimensions, angiosperms reach their phenotypic response limits on average at 740 ppm and conifers on average at 1,250 ppm CO_2. Further, our simulations predict that doubling today's CO_2 will decrease the annual transpiration flux of subtropical vegetation in Florida by ≈60 W·m^{-2}. We conclude that plant adaptation to rising CO_2 is altering the freshwater cycle and climate and will continue to do so throughout this century.

climate change | physiological forcing | plant evolution

Plants respond to the complex of environmental signals they perceive by plastic changes in their phenotype to increase individual fitness (1). The most apparent environmental change that induces phenotypic adaptations in plants is the global increase in atmospheric CO_2 concentration (CO_2) (2). In response to this rise in CO_2, plants reduce the diffusive stomatal conductance of their leaves [g_s (mol·m^{-2}·s^{-1})] to increase drought resistance (3) and reduce physiological costs associated with water transport (4). Plants can reduce g_s by dynamically closing their stomata within minutes (5, 6), and structurally within the lifespan of an individual by growing leaves with altered stomatal density [D (number of stomata·m^{-2})] and pore size at maximal stomatal opening [a_{max} (m^2)] (7, 8). Structural adaptations thereby reduce maximal stomatal conductance [g_{smax} (mol·m^{-2}·s^{-1})], which critically reduces actual g_s, especially when stomata are fully open during times with ample light and water (9).

Reduction of g_s via structural adaptation of g_{smax} has the potential to reduce transpiration fluxes and, thus, cause land surface warming in addition to changes in the global hydrological cycle with rising CO_2 (10). This climatic effect is termed the physiological forcing of CO_2, which acts beside and independent of its radiative forcing. Despite advances to quantify this physiological forcing with global climate models (11, 12), these models rely on semiempirical relations to simulate g_s from environmental variables (13, 14). Alternative models have been proposed on the mechanism that stomatal adaptations optimize carbon gain under the constraint of a cost of water loss (15, 16). Because of their mechanistic representation of stomatal responses, optimization models are potentially suitable to simulate canopy gas exchange under changing CO_2. However, optimization models implicitly assume that plants will continue to adapt g_s optimally to future rises in CO_2. Whether this assumption holds for the current rate of CO_2 increase is unknown, but structural stomatal responses might be constrained by limits to phenotypic plasticity (17, 18) and diffusion through stomatal pores (19).

To quantify physiological forcing of CO_2 on past and future climate, two challenges must therefore be addressed. First we test if the observed structural adaptation of g_{smax} to rising CO_2 can be explained by optimization of carbon gain under the constraint of a cost of water loss and second we predict at what level of CO_2 this structural adaptation ceases due to limits to phenotypic plasticity.

Recent advances in stomatal modeling provide possibilities to tackle the first challenge, because the hypothesis that plants adapt g_{smax} structurally to rising CO_2 to optimize carbon gain with water loss can be solved mathematically (15, 16). However, limited experimental data are available for model validation because experiments are generally too short to measure structural stomatal adaptation in forests that take decades or longer to fully adapt to elevated CO_2 (20). A unique dataset provides measurements of structural adaptation of g_{smax} to the CO_2 rise of the past century in eight C3 canopy species from natural subtropical vegetation in Florida (see Table 1 for species names) (8). Because these species are representative for vegetation in subtropical climates, these observations are crucial to validate models of stomatal adaptations for this climate zone.

The second challenge is more difficult to overcome because ideally species-specific limits to structural adaptation are observed in natural vegetation under rising CO_2. However, no historic analog of the current high rate of CO_2 increase can be found in the 400-million-year history of vascular plants (21, 22). The fossil record shows that CO_2 has been driving genetic adaptation that allowed plants to develop ranges of phenotypic plasticity to optimize functioning under changing CO_2 (22, 23). Despite these shifts in phenotypic plasticity at geologic timescales, structural adaptation of g_{smax} was always constrained by interdependence of D and a_{max} in the form of a power law relationship (Fig. 1*A*). Although D and a_{max} are not the only variables to determine g_{smax}, the constraint on their combined values does control the range of g_{smax}, which is calculated as (23):

Author contributions: H.J.d.B., F.W.-C., D.L.D., M.J.W., and S.C.D. designed research; H.J.d.B., E.I.L., and S.C.D. performed research; H.J.d.B., E.I.L., and F.W.-C. analyzed data; and H.J.d.B., E.I.L., and S.C.D. wrote the paper.

The authors declare no conflict of interest.

Freely available online through the PNAS open access option.

[1]To whom correspondence may be addressed. E-mail: h.deboer@geo.uu.nl or dilcher@indiana.edu.

This article contains supporting information online at www.pnas.org/lookup/suppl/doi:10.1073/pnas.1100555108/-/DCSupplemental.

Table 1. Species-specific limits of structural stomatal adaptations to rising CO_2

Species	g_{low}, mol·m^{-2}·s^{-1}	CO_{2lim}, ppm
Angiosperm average	0.76	740
Acer rubrum (Ar)	0.69	830
Ilex cassine (Ic)	0.46	770
Myrica cerifera (Mc)	0.73	670
Quercus laurifolia (Ql)	0.95	635
Quercus nigra (Qn)	0.97	775
Conifer average	0.31	1,250
Pinus elliottii (Pe)	0.19	1,465
Pinus taeda (Pt)	0.46	1,060
Taxodium distichum (Td)	0.29	1,210

Species-specific limits of the structural stomatal adaptation to rising CO_2, denoted by the lower limit on g_{smax} (defined as g_{low}) and CO_2 when mean g_{smax} reaches g_{low} (defined as CO_{2lim}).

$$g_{smax} = \frac{\frac{d_w}{v} \cdot D \cdot a_{max}}{l + \frac{\pi}{2}\sqrt{a_{max}/\pi}}, \quad [1]$$

where d_w (m^2·s^{-1}) is the diffusivity of water vapor and v (m^3·mol^{-1}) is the molar volume of air. The a_{max} is approximated from pore length [L (m)] on the premise that species studied here have ellipse-shaped apertures at a_{max} with width $W = L/2$. Pore depth l (m) is calculated from a species-specific relation with guard cell width and pore length (8) (Table S1). Note that g_s and g_{smax} are expressed as conductance to water vapor (mol·m^{-2}·s^{-1}). Additionally, D and a_{max} together express the percentage of leaf surface area allocated to stomatal pores as: $A_{\%} = 100 \cdot D \cdot a_{max}$. Fig. 1*A* shows how combined values of D and a_{max} relate to values of equal g_{smax} and equal $A_{\%}$, which is distributed lognormally (Fig. 1*B*).

The lognormal distribution of $A_{\%}$ allows for the estimation of species-specific limits to structural adaptation of g_{smax}, because $A_{\%}$ is bounded on the lower side by a generic value of 0.6% independent of g_{smax}, defined as $A_{\%low}$ (Fig. 1*B*). Although the species independent power law relationship between D and a_{max} is bound by $A_{\%low}$, each species uses a specific strategy to reduce g_{smax} linearly with $A_{\%}$ (Fig. 1*C*). So, if a species were to decrease g_{smax} indefinitely, $A_{\%}$ would eventually surpass $A_{\%low}$ and fall beyond the range of historic observations. We therefore suggest that structural response limits are determined by consistent species-specific strategies to reduce g_{smax} via adaptation of D and a_{max} along the linear relation between g_{smax} and $A_{\%}$, until $A_{\%low}$ is reached.

With a mechanistic model of stomatal adaptation and an empirical method to estimate response limits at hand, we can now quantify the physiological forcing of past and future CO_2 in a subtropical climate at a decadal to centennial timescale. We first model how stomatal optimization reduces g_{smax} with rising CO_2 and validate these results against observations of eight C3 canopy species (8) that responded structurally to the CO_2 rise of the past century. Because we suggest that these adaptations are constrained by limits to phenotypic plasticity, we derive the upper limits for each species in terms of CO_2. Finally, we use the stomatal optimization model with structural response limits to calculate physiological forcing of CO_2 rising from preindustrial (280 ppm) through present (385 ppm), and up to double present levels (770 ppm).

Results

Our simulations of stomatal optimization are consistent with observations that report a 17–55% decrease in g_{smax} from preindustrial to present CO_2 (Fig. 2) (8). Our model simulates g_{smax} for all species within the variability of observed g_{smax} (Fig. 2, *Inset*) as a consequence of adaptations to the complex of environmental factors determining D and a_{max}, including CO_2 (Fig. S1) (24). Although not all variability in observed g_{smax} can be explained from adaptation to CO_2, the consistent decreases of g_{smax} observed at decadal to centennial timescales are accurately reproduced by our model. These results indicate that structural adaptations of g_{smax} to CO_2 rising from preindustrial to present levels can be explained from optimization of carbon gain under the constraint of a cost of water loss.

Furthermore, our simulations show that g_{smax} continues to decrease with CO_2 rising beyond present values (Fig. 2). Interpreting these model results, we find this ongoing decrease in

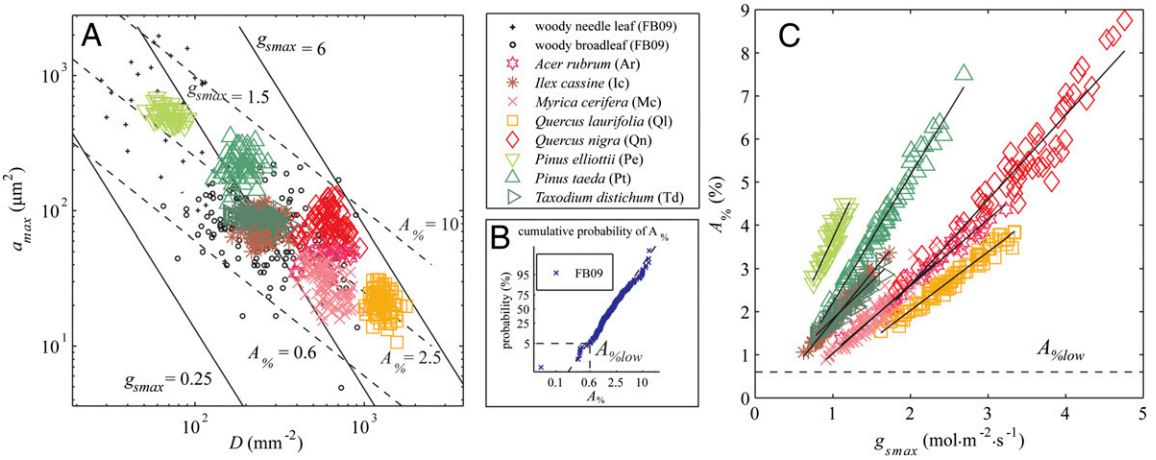

Fig. 1. An overview of observed relationships among stomatal density (D), pore size at maximal stomatal opening (a_{max}), and the resulting maximal stomatal conductance (g_{smax}) and leaf surface area allocated to stomatal pores at a_{max} ($A_{\%}$). (*A*) Power law relationship between D and a_{max} are plotted together with lines of equal g_{smax} (solid lines) and $A_{\%}$ (dashed lines). See Eq. **1** and Table S1 for calculations of g_{smax}. Note that logarithmic axes are used. (*B*) Cumulative probability of $A_{\%}$ for woody angiosperm and conifer species fitted to a lognormal distribution. The value of 0.6 indicates the estimated lower bound (5% probability) on $A_{\%}$ defined here as $A_{\%low}$. Note that a logarithmic x axis is used. (*C*) Species-specific strategies to adapt g_{smax} linearly with $A_{\%}$. The dashed line denotes $A_{\%low}$. Lines of linear least squares regressions are indicated per species and used to determine the intersect with $A_{\%low}$ to predict the lowest attainable g_{smax} for each species, defined as g_{low}. The r^2 values are: 0. 97 (Ar), 0.96 (Ic), 0.86 (Mc), 0.96 (Ql), 0.91 (Qn), 0.85 (Pe), 0.98 (Pt), and 0.94 (Td) with $P < 0.001$ for all. Data FB09 are from ref. 23, others from ref. 8. Species names and their abbreviations are defined in the legend.

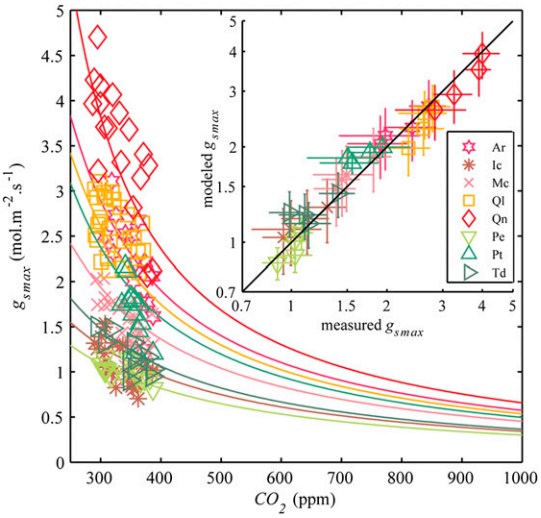

Fig. 2. Modeled structural adaptations of g_{smax} to CO_2 for each species (solid colored lines), compared with measured g_{smax} averaged at each measured CO_2. *Inset* shows a direct comparison between modeled and measured g_{smax} averaged over CO_2 quartiles of the data. Error bars indicate SDs of modeled (vertical) and measured (horizontal) g_{smax} in each quartile.

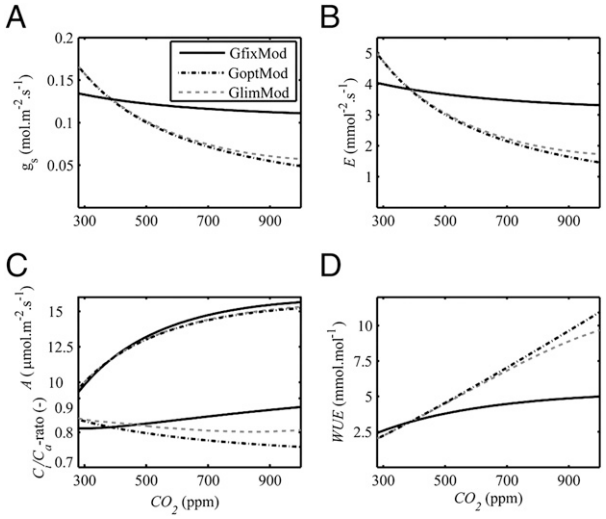

Fig. 3. Modeled daily average gas exchange at the leaf level for ensembles with dynamic stomatal adaptation only (GfixMod), with structural and dynamic adaptation (GoptMod) and with CO_2 response limits included (GlimMod). (*A*) Simulated stomatal conductance (g_s). (*B*) Transpiration (E). (*C*) Assimilation (A) and C_i/C_a-ratio at maximum photosynthesis. (*D*) Water use efficiency (*WUE*) expressed in [mmol (CO_2)·mol $(H_2O)^{-1}$].

g_{smax} unlikely because with the current rate of CO_2 increase, plants are likely to reach the limits of their phenotypic plasticity (17, 18, 25). We therefore predict structural response limits on the premise that the species-specific adaptation strategies observed remain unchanged at elevated CO_2 and will eventually be limited by $A_{\%low}$ at the lowest attainable g_{smax}, defined here as g_{low} (Fig. 1*C*). With our simulations of structural adaptation, we predict that values of g_{low} will be reached in a CO_2 range between 635 and 1,465 ppm (Table 1). Consistent with observations of stomatal adaptations at evolutionary timescales (23), the angiosperms in our dataset (Ar, Ic, Mc, Ql, and Qn) have notably lower response limits than conifers (Pe, Pt, and Td) (740 and 1,250 ppm CO_2 on average, respectively). This difference might be related to the distinct leaf vascular designs of angiosperms and conifers, which are intrinsically linked to the gas exchange capacity of their leaves (4). Angiosperms evolved toward densely veined leaves, which require highly conductive leaf surfaces with many small stomata to maximize gas exchange under low CO_2 (26). Contrastingly, conifers have less conductive leaf surfaces with fewer and larger stomata, matching the lower water transport capacity of the simpler leaf vascular design suited for higher CO_2 (27).

Structural stomatal adaptations potentially alter photosynthesis and canopy gas exchange because g_{smax} crucially constrains g_s, especially when assimilation rates reach their daily maximum and stomata are fully open. To determine how photosynthesis and leaf gas exchange is altered by structural stomatal adaptation, we perform three model ensemble simulations: one with dynamic adaptation superimposed on constant preindustrial g_{smax} (GfixMod), one with structural and dynamic adaptation (GoptMod), and one with CO_2 response limits imposed at g_{low} (Table 1) (GlimMod), each of which consists of eight species members.

The differences in simulated g_s between GfixMod, and GoptMod and GlimMod ensemble averages show that structural adaptation of g_{smax} constrains daily average g_s (Fig. 3*A*). From preindustrial to present CO_2, daily average g_s decreases by 20% in the GlimMod and GoptMod ensembles and by 5% in the GfixMod ensemble. From present to double CO_2, g_s decreases by 40% in the GlimMod and GoptMod ensembles and by 10% in the GfixMod ensemble. Because transpiration (E) is controlled by g_s and humidity deficit in the lower atmosphere, E decreases in line with g_{smax} at increasing CO_2, with 1.0 mmol·m^{-2}·s^{-1} from preindustrial to present, and 1.8 mmol·m^{-2}·s^{-1} from present to double CO_2 in the GlimMod and GoptMod ensembles (Fig. 3*B*). The GfixMod ensemble shows considerably less change in E, with 0.15 and 0.35 mmol·m^{-2}·s^{-1} from preindustrial through present to double CO_2, because only dynamic adaptation reduces g_s, whereas g_{smax} remains at its preindustrial value in this model ensemble.

Contrasting the large differences in transpiration among the three ensemble runs, it is clear that they all show a similar increase in assimilation (A) from 9 µmol·m^2·s^{-1} at preindustrial CO_2 to 15 µmol·m^2·s^{-1} at double CO_2 (Fig. 3*C*). The similarity in A increase indicates that g_{smax} does not strongly control A, but rather that A is controlled by CO_2 via changes in leaf interior CO_2 concentrations (C_i) (Fig. 3*C* shows the ratio of internal to atmospheric CO_2 concentration, or C_i/C_a-ratio). C_i therefore increases in line with CO_2 in the GfixMod ensemble and remains relatively constant over a wide range of CO_2 levels in the GoptMod and GlimMod ensembles. The latter response is commonly observed in C3 species and protects these plants from the adverse effects of photorespiration at low CO_2, whereas it increases the ratio of water loss versus carbon gain (termed water-use efficiency or *WUE*) with rising CO_2 (Fig. 3*D*) (28). These changes in C_i/C_a-ratio underline the advantage plants gain from adapting stomatal conductance in response to CO_2 (4).

The strength of physiological forcing ultimately depends on the change of canopy transpiration (ΔLE) under rising CO_2. When stomatal adaptations occur at the canopy scale, reduced leaf level transpiration might reduce humidity in the lower atmosphere and, in turn, increase transpiration due to an increased humidity gradient. To determine how transpiration is altered by structural stomatal adaptation, we upscale our stomata model to the canopy scale and include the feedback with moisture in the lower atmosphere. With this canopy scale model, we repeat the GfixMod, GoptMod, and GlimMod ensembles and estimate physiological forcing of the CO_2 rise from preindustrial to present levels and of doubling current CO_2.

The GoptMod and GlimMod ensembles both show a ΔLE of −30 W·m^{-2} due to the CO_2 rise from preindustrial to present levels and a ΔLE of −60 W·m^{-2} if CO_2 doubles (Fig. 4). The GfixMod ensemble includes only the effects of dynamic adap-

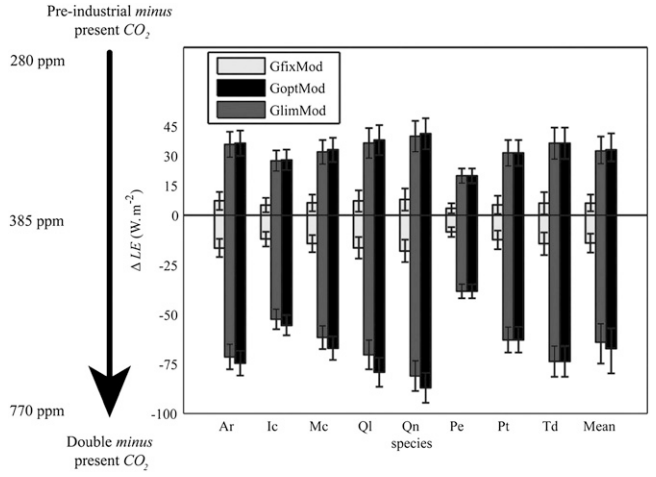

Fig. 4. Changes in annual canopy transpiration [ΔLE (W·m^{-2})] among preindustrial, present, and double CO_2 for ensembles with dynamic stomatal adaptation only (GfixMod), with structural and dynamic adaptation (GoptMod), and with CO_2 response limits included (GlimMod). Error bars for individual species denote SDs in daily average transpiration for preindustrial and double CO_2; error bars for mean values denote SDs between species averages.

tation, so here ΔLE is just −15 W·m^{-2} from preindustrial to double CO_2. The angiosperms in our dataset (Ar, Ic, Mc, Ql, and Qn) reach their response limits between 635 and 830 ppm CO_2 (Table 1), so ΔLE is slightly less (5 W·m^{-2}) in the GlimMod compared with GoptMod ensemble at double CO_2. The conifers in our dataset (Pe, Pt, and Td) reach their response limits at higher CO_2 (1,250 ppm on average) and, therefore, show no difference in ΔLE between the GlimMod and GoptMod ensembles. These results suggest that structural stomatal adaptations exert a continuing physiological forcing on climate.

Discussion

We confirm that structural adaptations of g_{smax} exert strong control on dynamic responses of g_s and thereby significantly reduce the annual transpiration flux from natural subtropical vegetation in Florida under rising CO_2. Our hypothesis is supported by model simulations based on optimization of carbon gain under the constraint of a plant physiological cost of water loss that reproduce the observed adaptation of g_{smax} (which decreased with 17–55% from preindustrial to present CO_2) (8). We further expect that plants will continue to adapt structurally until they reach the limits of their phenotypic plasticity. Because CO_2 is likely doubled by the end of this century (29) and response limits are generally reached around or above double present CO_2 levels, structural stomatal adaptation in subtropical vegetation will continue to amplify the climatic forcing of CO_2 throughout this century.

Our simulations with the stomatal optimization model predict that a doubling of present CO_2 will decrease the annual transpiration flux from subtropical vegetation in Florida by ≈60 W·m^{-2}. This decrease is considerable because the current annual evapotranspiration flux in Florida is ≈120 W·m^{-2} and transpiration constitutes ≈50% of this total (12, 30). Feedbacks at regional and continental scale could potentially compensate for reduced canopy transpiration and shift the fractional contribution away from transpiration (31). Accounting for these feedbacks and the contribution of transpiration to total surface latent heat flux, a comparable decrease in latent heat flux of 30 W·m^{-2} has been simulated over subtropical forests with the Hadley Centre global climate model (11, 32), which uses a semiempirical stomatal response model (13). The finding that stomatal adaptations are reducing canopy transpiration is supported by independent empirical data from river runoff that suggest reduced continental scale evapotranspiration over the past century (33). We therefore conclude that plant adaptation to CO_2 is altering the hydrological cycle and climate and will continue to do so under further rising CO_2.

Despite this evidence for the climatic effects of stomatal adaptations, changes in transpiration could be compensated if forests respond to rising CO_2 by growing taller and denser and, thus, increase leaf area index (LAI) (34). However, in dense subtropical forests, self-shading and down-regulation of photosynthetic capacity often limits this effect of CO_2 fertilization (35), so only forest-floor species are likely to benefit from rising CO_2 and these have little impact on canopy transpiration (36). Moreover, increased photosynthesis might also increase turnover rates, leading to a more dynamic forest with unchanged biomass and LAI (37). Simulations with a global vegetation model, which takes these considerations into account, indicate that in subtropical forests LAI increases by a maximum of 10% after a doubling of CO_2 (38). This marginal increase in LAI increases canopy transpiration by ≈5%, which is not sufficient to compensate for reduced transpiration at the leaf level. Decreased transpiration is therefore a robust response to increasing CO_2 in subtropical forests.

To estimate physiological forcing due to future CO_2 increase, it is essential to validate response limits to structural adaptation. We based estimates of response limits on the hypothesis that plant species adapt g_{smax} by altering D and a_{max} until they reach a generic value of $A_{\%low}$. Although the physiologic relevance of $A_{\%low}$ is not yet fully understood, it might represent a tradeoff between leaf interior CO_2 transport and the structural costs associated with the required leaf water transport system (4, 39). Because angiosperms and conifers have different leaf hydraulic systems (27), it could be argued that they also have different limits on $A_{\%}$ and that a generic $A_{\%low}$ overestimates phenotypic plasticity for either growth type (17, 40). However, our analysis does not show significant differences in the lower ranges of $A_{\%}$ between angiosperms and conifers (Fig. S2). Therefore, we cannot reject the hypothesis that $A_{\%low}$ is a generic lower limit of $A_{\%}$ and, thus, the use of equal $A_{\%low}$ for angiosperms and conifers is appropriate. Response limits based on $A_{\%low}$ might therefore represent upper limits of ambient CO_2 to which the design of the water transport system of each species is optimized. Our prediction indicates that response limits are lower for angiosperms than for conifers (on average 740 and 1,250 ppm CO_2, respectively), roughly reflecting the ambient CO_2 under which these lineages evolved (41, 42).

Comparable differences in stomatal adaptation between angiosperms and conifers have been noted in free-air carbon enrichment (FACE) and greenhouse experiments under elevated CO_2 (28, 43). These studies indicate that angiosperms respond with a higher sensitivity in g_s to elevated CO_2 than conifers. Our results suggest that differences in CO_2 response could result from the plant physiological cost of water loss, represented by the Lagrangian multiplier (λ) (Table S2) in the optimization procedure (15). According to the optimization hypothesis, angiosperm species with a low λ can resort to high values of g_{smax} to function under low CO_2, whereas conifer species with a high λ cannot. Conversely, a rise in CO_2 reverses this adaptation and, therefore, shows an (initial) stronger response in angiosperms than conifers. However, because conifers are expected to have higher response limits than angiosperms, they might continue to optimize g_{smax} at CO_2 levels when angiosperms have reached their limit of phenotypic plasticity.

Because CO_2 is rising at exceptional rates, plants face the challenge of increasing individual fitness with plastic responses in their phenotype. Although modern plants have adapted their physiology to the historically low CO_2 by increasing the diffusive conductance of their leaves over the past million years, the cur-

rent rise in CO_2 allows a reversal of this adaptation (23). Reducing maximum leaf conductance under rising CO_2 makes individual plants more productive and drought resistant but also has the climatic consequence of reduced transpiration and associated changes in surface energy balance and the hydrological cycle (10, 33). With CO_2 continuing to increase, it is crucial to estimate the global magnitude of this climatic forcing via plant physiological responses and the two-way coupling between vegetation and climate (44, 45). Furthermore, the ongoing rise in CO_2 might give competitive advantage to plant lineages that evolved under high CO_2 and, thereby, allow a shift of existing vegetation composition favoring plant lineages tied to an earlier time (25).

Model Equations

A biochemical model of photosynthesis (46) is used to simulate assimilation of CO_2 [A (mol·m^{-2}·s^{-1})]:

$$A = \left(1 - \frac{\Gamma}{C_i}\right) \cdot \min(W_c, W_j) - R_d \quad [2]$$

with

$$W_c = V_{cmax} \frac{C_i}{C_i + K_c\left(1 + \frac{p_0}{K_0}\right)}, W_j = \frac{2}{9} J \frac{C_i}{C_i + \frac{7}{3}\Gamma} \quad [3]$$

in which Γ (mol·mol^{-1}) is the CO_2 compensation point in absence of dark respiration R_d (mol·m^{-2}·s^{-1}), C_i (mol·mol^{-1}) is the intercellular CO_2 concentration, W_c and W_j (mol·m^{-2}·s^{-1}) are the Rusbisco and RuBP limited rates of carboxylation, V_{cmax} (mol·m^{-2}·s^{-1}) is the maximum carboxylation capacity, K_c (mol·mol^{-1}) and K_o (mol·mol^{-1}) are the Michaelis-Menten constants for carboxylation and oxygenation and p_o (mol·mol^{-1}) is the partial pressure of oxygen. The rate of electron transport [J (mol·m^{-2}·s^{-1})] depends on the photon flux density [Q (mol·m^{-2}·s^{-1})], the rate and maximum rate of electron transport (15) and temperature response of photosynthesis parameters (47). Furthermore, V_{cmax} and J_{max} exhibit down-regulation in response to rising CO_2 (22) (see *SI Text* for details on parameter values).

Structural stomatal adaptations to changes in atmospheric CO_2 concentrations [CO_2 (mol·mol^{-1})] are simulated from optimization of carbon gain under the constraint of a plant physiological cost of water loss (15). The underlying assumption of this approach is that plants cannot transpire more water than they can transport from the soil, through their roots and stem up to their leaves (48). As maximum transpiration generally occurs during maximum photosynthesis, this model calculates an optimal g_{smax} [defined as g_{sopt} (mol·m^{-2}·s^{-1})] according to daily maximum photosynthesis and water availability at this time:

$$g_{sopt} = \left\{ \sqrt{\frac{q(K+\Gamma)[CO_2(q-R_d) - (q\Gamma + KR_d)]}{(CO_2 + K - \lambda a w_d)\lambda a w_d}} \times (CO_2 + K - 2\lambda a w_d) + (q - R_d)CO_2 - (q\Gamma + KR_d) - q(K+\Gamma) \right\} \frac{a}{(CO_2 + K)^2} \quad [4]$$

in which:

$$q = \begin{cases} V_{cmax} & \text{if } W_c \le W_j \\ \frac{2}{9}J & \text{if } W_c > W_j \end{cases}, \quad K = \begin{cases} K_c\left(1 + \frac{p_o}{K_o}\right) & \text{if } W_c \le W_j \\ \frac{7}{3}\Gamma & \text{if } W_c > W_j \end{cases} \quad [5]$$

and the Lagrangian multiplier [λ (mol·mol^{-1})] represents a species specific empirical constant for the cost of water loss (Table S2), w_d (mol·mol^{-1}) is the water vapor deficit calculated from relative and saturated atmospheric humidity [w_{rel} (-) and w_{sat} (mol·mol^{-1})] as $w_d = w_{sat}(1 - w_{rel})$ and a (-) is the ratio between diffusivity of water vapor and CO_2 vapor [d_w and d_c (m^2·s^{-1})]. Saturation value of water vapor and diffusivities of CO_2 and water vapor are calculated depending on ambient temperature (15, 49).

We obtain g_{smax} for every 5 ppm CO_2 interval from 280 to 2,000 ppm from maximum g_{sopt} by prescribing an average diurnal cycle of environmental boundary conditions for the season when leaves are formed (March, April, and May in Florida). Meteorological data are obtained from the AmeriFlux database (50) (Fig. S1). For each species, λ is calibrated on the highest CO_2 quartile of species-specific g_{smax} observations.

Dynamic stomatal responses are simulated with a stomatal response model (51) superimposed on the model of structural adaptation. This model simulates dynamic adaption of g_s to environmental boundary conditions from changes in osmotic gradients in guard cells as a function of water availability and photosynthesis. Simulated actual g_s is the product of g_{smax} and the closure related to guard cell turgor [f_t (-)]:

$$g_s = g_{max} f_t, \quad \text{with } f_t = \frac{\alpha - \gamma}{\alpha + K_g} \quad [6]$$

in which γ (-) is the hydroactive compensation point, K_g (-) is the Michaelis constant for the guard cell advantage [α (-)], which is calculated as a function of guard cell turgor related to water availability and photosynthesis (51).

To solve the model for leaf level gas exchange, we first obtain values for g_{smax} at each CO_2 level and then force the dynamic and structural adaptation models with a diurnal cycle of annual average environmental boundary conditions (Fig. S1).

We upscale the leaf level simulations to canopy scale by considering photosynthesis at different heights in the canopy and the feedback between transpiration and moisture in the lower atmosphere. Differences in light conditions within the canopy are simulated from light interception using a simple exponential light decay scheme (Beer's law) over 5 layers of equal LAI (52):

$$Q(L_c) = Q(0)e^{-kL_c}, \quad [7]$$

where $Q(L_c)$ (mol·m^{-2}·s^{-1}) is the photosynthetically active radiation calculated from cumulative LAI [L_c (-)] above the considered location in the canopy, photosynthetically active radiation at the canopy top $Q(0)$ and the light extinction coefficient k (-). Feedback between transpiration and moisture in the lower atmosphere is included considering moisture redistribution in the planetary boundary layer (53).

To solve the model for canopy scale gas exchange over 1 y, the humidity of the upper atmosphere is iteratively calculated by forcing the model with an annual cycle of environmental boundary conditions (Fig. S1). Then, g_s and E are calculated for every CO_2 level in each layer of the canopy.

Because A depends on the total leaf conductance [g_t (mol·m^{-2}·s^{-1})] but, in turn, controls g_s, C_i is expressed as a function of CO_2, A and g_t:

$$C_i = CO_2 - \frac{Aa}{g_t}, \text{ with } g_t^{-1} = g_{bl}^{-1} + g_s^{-1} + g_i^{-1}, \quad [8]$$

where g_{bl} (mol·m^{-2}·s^{-1}) is the conductance of the leaf boundary layer (54) and g_i (mol·m^{-2}·s^{-1}) is the internal conductance, defined here as $g_i = \frac{1}{2} g_s$ (39).

ACKNOWLEDGMENTS. The manuscript was improved by comments from Henk Visscher, Brian Dermody, Max Rietkerk, and two reviewers. We thank Wilfried Konrad for his helpful suggestions on modeling stomatal responses. This research is Netherlands Research School of Sedimentary Geology publication no. 20110102 and was partly funded by the High Potential project of Utrecht University.

1. Trewavas A (2009) What is plant behaviour? *Plant Cell Environ* 32:606–616.
2. Hetherington AM, Woodward FI (2003) The role of stomata in sensing and driving environmental change. *Nature* 424:901–908.
3. Cowan IR, Farquhar GD (1977) Stomatal function in relation to leaf metabolism and environment. *Symp Soc Exp Biol* 31:471–505.
4. Beerling DJ, Franks PJ (2010) Plant science: The hidden cost of transpiration. *Nature* 464:495–496.
5. Darwin F (1898) Observations on stomata. *Proc R Soc Lond* 63:413–417.
6. Farquhar GD, Sharkey TD (1982) Stomatal conductance and photosynthesis. *Annu Rev Plant Physiol* 33:317–345.
7. Royer DL (2001) Stomatal density and stomatal index as indicators of paleoatmospheric CO(2) concentration. *Rev Palaeobot Palynol* 114:1–28.
8. Lammertsma EI, de Boer HJ, Dekker SC, Dilcher DL, Lotter AF, Wagner-Cremer F (2011) Global CO2 rise leads to reduced maximum stomatal conductance in Florida vegetation. *Proc Natl Acad Sci USA* 108:4035–4040.
9. Wullschleger SD, Tschaplinski TJ, Norby RJ (2002) Plant water relations at elevated CO2 — implications for water-limited environments. *Plant Cell Environ* 25:319–331.
10. Betts RA, et al. (2007) Projected increase in continental runoff due to plant responses to increasing carbon dioxide. *Nature* 448:1037–1041.
11. Andrews T, Doutriaux-Boucher M, Boucher O, Forster P (2010) A regional and global analysis of carbon dioxide physiological forcing and its impact on climate. *Clim Dyn*, 10.1007/s00382-010-0742-1.
12. Cao L, Bala G, Caldeira K, Nemani R, Ban-Weiss G (2010) Importance of carbon dioxide physiological forcing to future climate change. *Proc Natl Acad Sci USA* 107:9513–9518.
13. Ball JT, Woodrow IE, Berry A (1987) *Progress in Photosynthesis Research* (Martinus Nijhoff, Dordrecht, The Netherlands), Vol IV.
14. Leuning R (1995) A critical appraisal of a combined stomatal-photosynthesis model for C3 plants. *Plant Cell Environ* 18:339–355.
15. Konrad W, Roth-Nebelsick A, Grein M (2008) Modelling of stomatal density response to atmospheric CO2. *J Theor Biol* 253:638–658.
16. Katul G, Manzoni S, Palmroth S, Oren R (2010) A stomatal optimization theory to describe the effects of atmospheric CO2 on leaf photosynthesis and transpiration. *Ann Bot (Lond)* 105:431–442.
17. Kürschner WM, Wagner F, Visscher EH, Visscher H (1997) Predicting the response of leaf stomatal frequency to a future CO2-enriched atmosphere: Constraints from historical observations. *Geol Rundsch* 86:512–517.
18. Ghalambor CK, McKay JK, Carroll SP, Reznick DN (2007) Adaptive versus non-adaptive phenotypic plasticity and the potential for contemporary adaptation in new environments. *Funct Ecol* 21:394–407.
19. Wynn JG (2003) Towards a physically based model of CO2-induced stomatal frequency response. *New Phytol* 157:394–398.
20. McMurtrie RE, Medlyn BE, Dewar RC (2001) Increased understanding of nutrient immobilization in soil organic matter is critical for predicting the carbon sink strength of forest ecosystems over the next 100 years. *Tree Physiol* 21:831–839.
21. Berner RA (2006) GEOCARBSULF: A combined model for Phanerozoic atmospheric O2 and CO2. *Geochim Cosmochim Acta* 70:5653–5664.
22. Franks PJ, Beerling DJ (2009) CO(2)-forced evolution of plant gas exchange capacity and water-use efficiency over the Phanerozoic. *Geobiology* 7:227–236.
23. Franks PJ, Beerling DJ (2009) Maximum leaf conductance driven by CO2 effects on stomatal size and density over geologic time. *Proc Natl Acad Sci USA* 106: 10343–10347.
24. Wagner-Cremer F, Donders TH, Visscher H (2010) Drought stress signals in modern and subfossil Quercus laurifolia (Fagaceae) leaves reflect winter precipitation in southern Florida tied to El Nino-Southern Oscillation activity. *Am J Bot* 97:753–759.
25. Ward JK, Kelly JK (2004) Scaling up evolutionary responses to elevated CO2: lessons from Arabidopsis. *Ecol Lett* 7:427–440.
26. Brodribb TJ, Feild TS (2010) Leaf hydraulic evolution led a surge in leaf photosynthetic capacity during early angiosperm diversification. *Ecol Lett* 13:175–183.
27. Brodribb TJ, Holbrook NM, Zwieniecki MA, Palma B (2005) Leaf hydraulic capacity in ferns, conifers and angiosperms: Impacts on photosynthetic maxima. *New Phytol* 165: 839–846.
28. Ainsworth EA, Rogers A (2007) The response of photosynthesis and stomatal conductance to rising [CO2]: Mechanisms and environmental interactions. *Plant Cell Environ* 30:258–270.
29. IPCC (2007) Contribution of Working Group I to the Fourth Assessment Report of the Intergovernmental Panel on Climate Change. Solomon S, et al. (eds). (Cambridge University Press, Cambridge, United Kingdom and New York, NY) 996 pp.
30. Douglas EM, Jacobs JM, Sumner DM, Ray RL (2009) A comparison of models for estimating potential evapotranspiration for Florida land cover types. *J Hydrol (Amst)* 373:366–376.
31. McNaughton K, Jarvis P (1991) Effects of spatial scale on stomatal control of transpiration. *Agric For Meteorol* 54:279–302.
32. Boucher O, Jones A, Betts R (2009) Climate response to the physiological impact of carbon dioxide on plants in the Met Office Unified Model HadCM3. *Clim Dyn* 32: 237–249.
33. Gedney N, et al. (2006) Detection of a direct carbon dioxide effect in continental river runoff records. *Nature* 439:835–838.
34. Norby RJ, et al. (2005) Forest response to elevated CO2 is conserved across a broad range of productivity. *Proc Natl Acad Sci USA* 102:18052–18056.
35. Millard P, Sommerkorn M, Grelet GA (2007) Environmental change and carbon limitation in trees: a biochemical, ecophysiological and ecosystem appraisal. *New Phytol* 175:11–28.
36. Naumburg E, Ellsworth DS (2000) Photosynthetic sunfleck utilization potential of understory saplings growing under elevated CO2 in FACE. *Oecologia* 122:163–174.
37. Malhi Y, et al. (2009) Exploring the likelihood and mechanism of a climate-change-induced dieback of the Amazon rainforest. *Proc Natl Acad Sci USA* 106:20610–20615.
38. Kergoat L, et al. (2002) Impact of doubled CO2 on global-scale leaf area index and evapotranspiration: Conflicting stomatal conductance and LAI responses. *J Geophys Res* 107:4808.
39. Warren CR (2008) Stand aside stomata, another actor deserves centre stage: The forgotten role of the internal conductance to CO2 transfer. *J Exp Bot* 59:1475–1487.
40. Strand JA, Weisner SEB (2004) Phenotypic plasticity—contrasting species-specific traits induced by identical environmental constraints. *New Phytol* 163:449–451.
41. Dilcher D (2000) Toward a new synthesis: Major evolutionary trends in the angiosperm fossil record. *Proc Natl Acad Sci USA* 97:7030–7036.
42. Henry RJ (2005) *Plant Diversity and Evolution: Genotypic and Phenotypic Variation in Higher Plants* (CABI Publishing, Oxon, UK).
43. Brodribb TJ, McAdam SAM, Jordan GJ, Feild TS (2009) Evolution of stomatal responsiveness to CO(2) and optimization of water-use efficiency among land plants. *New Phytol* 183:839–847.
44. Kleidon A (2004) Optimized stomatal conductance of vegetated land surfaces and its effects on simulated productivity and climate. *Geophys Res Lett* 31:L21203.
45. Dekker SC, et al. (2010) Biogeophysical feedbacks trigger shifts in the modelled vegetation-atmosphere system at multiple scales. *Biogeosciences* 7:1237–1245.
46. Farquhar GD, von Caemmerer S, Berry JA (2001) Models of photosynthesis. *Plant Physiol* 125:42–45.
47. Bernacchi CJ, Pimentel C, Long SP (2003) In vivo temperature response functions of parameters required to model RuBP-limited photosynthesis. *Plant Cell Environ* 26: 1419–1430.
48. Baldocchi DD, Xu L (2007) What limits evaporation from Mediterranean oak woodlands—The supply of moisture in the soil, physiological control by plants or the demand by the atmosphere? *Adv Water Resour* 30:2113–2122.
49. Nobel PS (1999) *Physicochemical and Environmental Plant Physiology* (Academic, San Diego).
50. Powell TL, et al. (2008) Carbon exchange of a mature, naturally regenerated pine forest in north Florida. *Glob Change Biol* 14:2523–2538.
51. Buckley TN, Mott KA, Farquhar GD (2003) A hydromechanical and biochemical model of stomatal conductance. *Plant Cell Environ* 26:1767–1785.
52. Jogireddy VR, Cox PM, Huntingford C, Harding RJ, Mecardo L (2006) *An Improved Description of Canopy Light Interception for Use in a GCM Land-Surface Scheme: Calibration and Testing Against Carbon Fluxes at Coniferous Forest. Hadley Centre Technical note 63* (The Hadley Centre, Exeter, UK).
53. McNaughton KG, Jarvis PG (1984) Using the Penman-Monteith equation predictively. *Agric Water Manage* 8:263–278.
54. Vesala T (1998) On the concept of leaf boundary layer resistance for forced convection. *J Theor Biol* 194:91–100.